Pressure-Driven Evolution of the Covalent Network in CaB_6

A. N. Kolmogorov,[1] S. Shah,[1] E. R. Margine,[1] A. K. Kleppe,[2] and A. P. Jephcoat[2,*]

[1]*Department of Materials, University of Oxford, Parks Road, Oxford OX1 3PH, United Kingdom*
[2]*Diamond Light Source, HSIC, Didcot, Oxfordshire OX11 0DE, United Kingdom*

(Received 30 March 2012; published 16 August 2012)

We synthesized and solved an unexpectedly complex crystal structure of CaB_6 under high pressures (up to 44 GPa) and temperatures. The only known crystal structure in the large family of metal hexaborides, a simple cubic *cP*7 type discovered over 80 years ago, is shown here to transform into a tetragonal *tI*56 configuration comprised of unfamiliar 24-atom boron units. The interpretation of the convoluted x-ray diffraction pattern was accomplished with an *ab initio* evolutionary search which identified the *tI*56 structure (28 atoms per primitive unit cell) without any parameter input. The exotic CaB_6 phase was successfully quenched down to ambient pressure.

DOI: 10.1103/PhysRevLett.109.075501 PACS numbers: 81.40.Vw, 61.66.Fn

Matter subjected to extreme pressures can exhibit surprising binding trends: single elements crystallize in incommensurate host-guest structures (Ba, Rb, Al) [1,2] and normally immiscible systems are expected to become compound-forming (Rb-B, Li-Be) [3,4]. High-pressure materials that remain (meta)stable under normal conditions, e.g., diamond or cubic boron nitride, are especially interesting as their outstanding properties can be utilized in practical applications [5]. Synthesis and characterization of new high-pressure polymorphs, such as γ-B_{28} [6–8] or *oC*88-Li [9], pose a number of challenges. Experimentally, the desired pressure (P)–temperature (T) conditions of order 50 GPa and 2000 K can be readily achieved in the laser-heated diamond anvil cell (DAC). However, the x-ray diffraction (XRD) data from polycrystalline samples of nanogram quantities is in most cases insufficient for determination and refinement of unknown large structures. Theoretically, a number of techniques have been proposed in the last few years for identification of unique (meta) stable crystal structures with only the composition as an input [7,10–15]. In practice, the particularly complex 28-atom γ-B_{28} [7] or the 44-atom *oC*88-Li [9] ground states consistent with powder XRD patterns were found using unit cell parameters extracted from the experimental XRD data.

The compound examined in this study, a semiconducting CaB_6, is a member of a large MB_6 family known for a range of properties and applications. For example, rare-earth hexaborides exhibit valence-fluctuations (SmB_6) and Kondo (CeB_6) effects or have low work functions and low volatility at high T (LaB_6, CeB_6) allowing their use as high-performance thermionic emitters [16]. YB_6 superconducts [17] at 7 K and CaB_6 can show weak ferromagnetism initially suspected to come from the free electron gas [18] but later argued to originate from defects [19]. To the best of our knowledge, only one crystal structure, *cP*7 [20], has been conclusively characterized in this M-B stoichiometry which can be represented by B_6 octahedra and metal ions arranged on the CsCl lattice (Fig. 1) (this lack of structural diversity is quite unusual for metal borides given the variety of boron network morphologies observed at other compositions [21]). Fine features in LaB_6 and CaB_6 powder diffraction patterns appearing around 10 GPa were better indexed with closely related orthorhombic unit cells [22,23] but were not reproduced in a recent LaB_6 [24] and the present CaB_6 studies. Instead, application of high pressure and temperature in our DAC experiments induced irreversible rebonding of the covalent network in CaB_6. Synchrotron XRD data indicated formation of multiple phases yielding no direct information about the unit cell parameters of the new phases and a low-enthalpy *tI*56-CaB_6 structure consistent with the XRD patterns was found through unconstrained optimization driven by an evolutionary algorithm (EA). We illustrate that for such large systems (28 atoms per primitive unit cell) the identification of a ground state truly 'from scratch' is possible but involves order(s) of magnitude more computation compared to the ground state searches with incorporated experimental information [7,9]. The ability of advanced optimization methods to handle systems of such size is essential in the exploration of compressed matter: while fairly simple structures can be often expected to form under high pressures [12], recent and present studies have shown appearance of configurations with large or nonintuitive unit cell sizes [7,10,14].

The inevitability of a structural transformation in CaB_6 under pressure was first predicted with our density functional theory analysis [25–29] which showed the compressed structure's thermodynamic and dynamical instability. Thermodynamically unstable structures can lower their Gibbs energy by transforming into more stable polymorphs or decomposing into other products. Dynamically unstable structures, in addition, have at least one phonon mode with imaginary frequency and thus have no activation barrier to go to corresponding nearby minima in the configuration space.

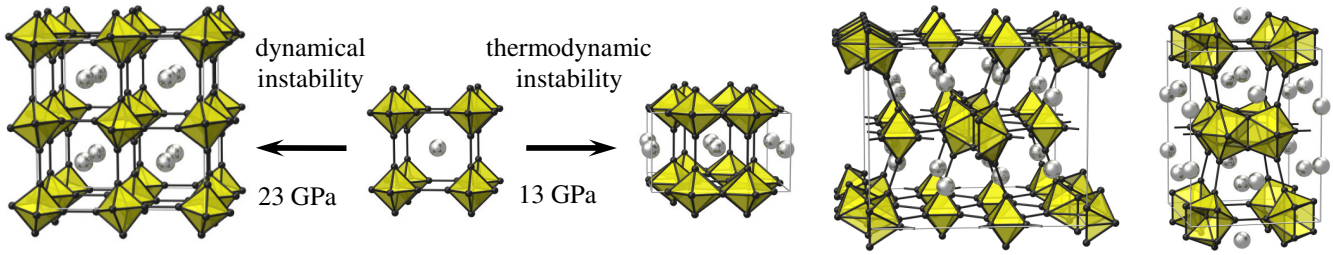

(a) oP28 (b) cP7 (Pm-3m) (c) oS28 (d) oS56 (e) tI56

FIG. 1 (color online). Competing high-pressure structures of CaB_6, the B and Ca atoms are shown as small black and large silver spheres, respectively. The known cubic structure ($cP7$ in Pearson notation, space group $Pm\bar{3}m$) is made out of boron octahedra. $oP28$ ($Pnma$) is one of the possible distortions of $cP7$. $oS28$ ($Cmmm$) is a metastable structure made out of twinned pentagonal bipyramids. $oS56$ ($Cmcm$) is our lowest enthalpy structure for 13–32 GPa pressures in which half of the boron octahedra opened up to form zig-zag strips. $tI56$ ($I4/mmm$), comprised of large 24-atom boron units, is a new ground state candidate above 32 GPa supported by x-ray data in the present study. The cell parameters are given in the Supplemental Material [31].

Linear response calculations of the $cP7$-CaB_6 phonon dispersion at 30 GPa revealed that a whole phonon branch involving rotation of rigid boron octahedra has, just as in YB_6 and MgB_6 [17,32], imaginary frequencies along the M-R direction in the Brillouin zone [33]. The linear behavior of ω^2 with pressure, an indication of the soft-mode phase transition described by Landau theory, allowed us to estimate the critical pressure to be 23 GPa for ω_R (25 GPa for ω_M). In order to understand the origin of the dynamical instability we calculated $\omega_M(P)$ dependences for all divalent metal hexaborides (Fig. 2) which showed clearly the importance of the metal size: one can think of the metal cations as space fillers "inflating" the boron framework. Ba and Sr are large enough to keep the structure from collapsing up to at least 60 GPa while Be and Mg are so small that the structure is dynamically unstable at zero pressure. Rotation of the B_6 units occurs naturally at the M_2B_6 composition in the Li-B system [34]. Construction of distorted $cP7$-based structures turned out to be difficult due to the presence of multiple soft modes but we identified three closely related dynamically stable structures, $oP28$ [Fig. 1(a)], $hR42$, and $tI28$, see Refs. [31,33].

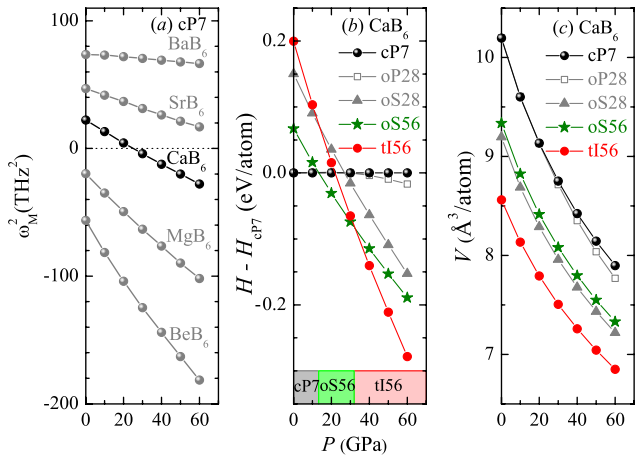

FIG. 2 (color online). Calculated properties of known ($cP7$) and predicted ($oP28$, $oS28$, $oS56$, and $tI56$) structures of CaB_6 as a function of pressure at $T = 0$ K [25,31]: (a) M-point phonon frequency in $cP7$ becoming imaginary above 25 GPa for CaB_6 in the divalent series (b) formation enthalpy at $T = 0$ K referenced to $cP7$ showing $cP7 \rightarrow oS56 \rightarrow tI56$ transformation at 13 and 32 GPa, respectively; (c) atomic volume.

In addition to being prone to distortions, $cP7$-CaB_6 was demonstrated to be thermodynamically unstable under compression through an unconstrained EA ground state search as implemented in the module for *ab initio* structure evolution (MAISE) [35]. The module is linked with VASP [27–29] and enables full structural optimization starting with random or known configurations by passing on beneficial traits from parents to offspring via crossover and mutation operations [31]. Our first extensive runs for CaB_6 unit cells up to 14 atoms suggested an orthorhombic $oS28$ structure [Fig. 1(c)] to be the lowest-enthalpy structure at 30 GPa, stabilizing over $cP7$ at 28 GPa.

The behavior of calcium hexaboride under pressure was studied in a series of experiments in which DACs were loaded with 150 μm-sized, 99% purity $cP7$-CaB_6. X-ray diffraction experiments were performed at Beamline I15, Diamond Light Source. We carried out nine separate loadings with different sample amounts and pressure media (argon or argon-helium). Key results were obtained in five sets of measurements: during a compression of CaB_6 from 2.7 to 28 GPa (DAC1) and after the laser-heating of CaB_6 at 16 GPa (DAC2), 31 GPa (DAC3), 34 GPa (DAC1), 44 GPa (DAC4) followed by decompression down to 14 GPa (DAC1) or 1 bar (DAC3). Representative diffraction patterns integrated with FIT2D [36] are shown in Fig. 3 with patterns at other pressures available in Ref. [31].

The compression of CaB_6 at room temperature (T) did not lead to the splitting of the (200) peak that signalled a cubic $\leftrightarrow$ orthorhombic transformation at around 12 GPa in a previous study [23]. Instead, the intensity of the (111) peak, normal at 1 bar or 2.7 GPa in our measurements, was greatly reduced in all the patterns collected for pressures

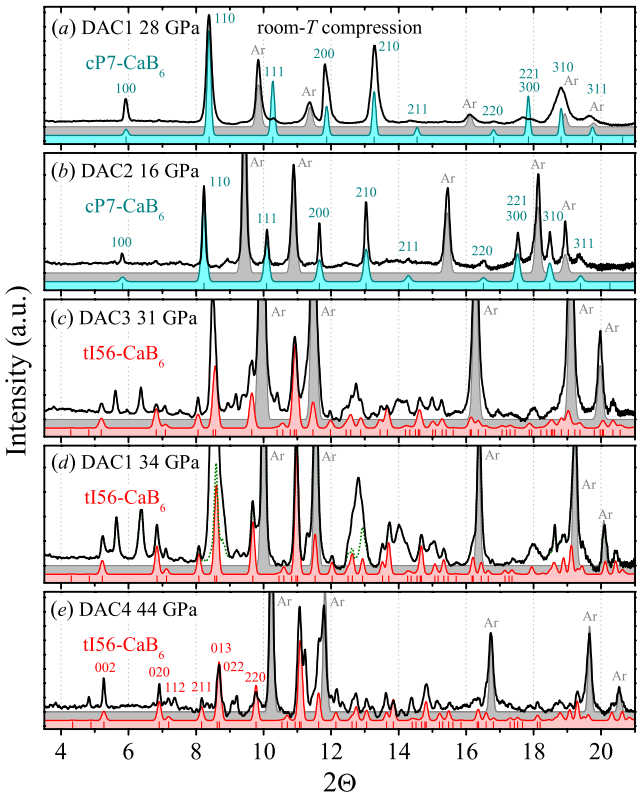

FIG. 3 (color online). Observed (thin lines) and simulated patterns (shaded areas) collected at room T and high pressures for CaB_6 after room-T compression (a) and laser-heating (b–d). The blue, red, and grey curves correspond to $cP7$-CaB_6, $tI56$-CaB_6, and fcc-Ar respectively. The green dotted line in (d) showing near 8.6 and 12.8 degrees corresponds to masked signal as described in the text. All the patterns were simulated with the lazy algorithm as implemented in the Inorganic Crystal Structure Database [37]; the used lattice parameters were refined via Le Bail fitting but remained close to the predicted ones (see Fig. S5 in Ref. [31]). All datasets are shown for $\lambda = 0.4084$ Å, see Fig. S6 in Ref. [31] for more details.

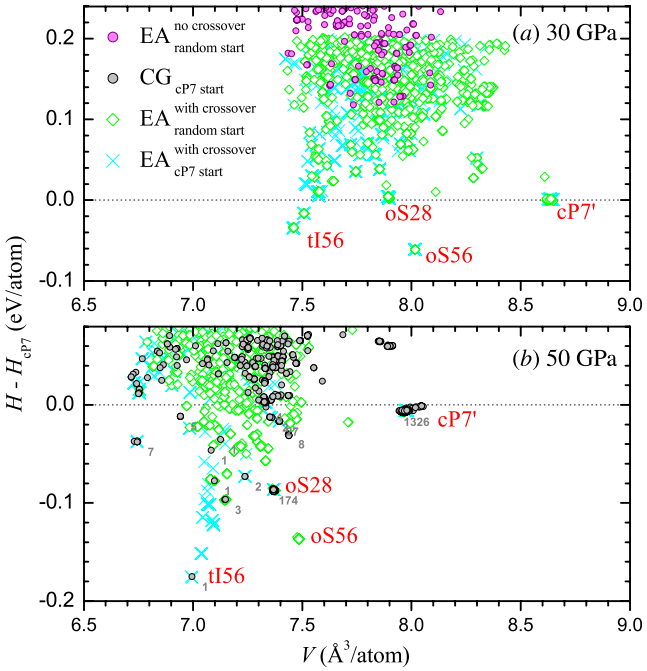

FIG. 4 (color online). Output of the ground state search for Ca_4B_{24} unit cells carried out with MAISE [35] linked to VASP [25,27–29] using different optimization strategies [31]. The populations were created either randomly (green hollow diamonds and magenta circles) or via distortion of $cP7$ supercells (cyan crosses and grey circles) as detailed in Ref. [31]. At both pressures, we carried out the evolutionary algorithm (EA)-driven searches with both crossover and mutation operations. At 30 GPa, an additional EA search was carried out with just the mutation operation. At 50 GPa, a nonevolutionary approach based on the local conjugate-gradient (CG) relaxation of distorted $cP7$ supercells was also able to produce the complex $tI56$ solution (the numbers in grey show how many times a particular structure was found in 10^4 tries). Note that $cP7$ is dynamically unstable above 23 GPa and close solutions are grouped as $cP7'$.

above 6.7 GPa; the origin of the (111) peak suppression is unclear as the possible rhombohedral distortion ($cP7$ to $hR42$) requires much higher (~ 23 GPa) pressures. The use of methanol-ethanol and argon pressure media delivering different anisotropic stresses in their solid forms is a likely reason for the different response of CaB_6 to applied pressure in the previous [23] and present experiments. In both cases, however, the lack of major changes in the x-ray patterns [Fig. 3(a)] indicates that CaB_6 retains its 3D morphology at room T up to at least 28 GPa. Patterns obtained after laser-heating the sample at 16 GPa [Fig. 3(b)] provide further support that $cP7$ structure remains at least metastable at this pressure as all low-angle peaks were recovered.

To promote rebonding in the strongly bound covalent boron network we laser-heated three CaB_6 samples at 31, 34, and 44 GPa [Figs. 3(c)–3(e)] and for the first time obtained conclusive evidence of a significant structural transformation for any metal hexaboride. The relation between the original $cP7$ and new phase(s) can be seen in the splitting of the (100) peak into two (at 31 and 34 GPa) or one (at 44 GPa) nearly symmetrical doublets. Indexing peaks is an important step towards solving the crystal structure [7] but application of a commonly used dichotomy algorithm [38] did not produce any solutions in our case. When the $oS28$ simulated pattern did not fit the observed ones it became evident that larger unit cells ought to be considered.

We used several strategies to locate the stablest configurations with MAISE at 30 and 50 GPa for 2, 3, and 4 CaB_6 formula units per primitive cell: from randomization and relaxation of $cP7$-CaB_6 supercells to various evolutionary search settings as described in Fig. 4 and Ref. [31]. 5×10^4 local conjugate-gradient (CG) structural optimizations with VASP were carried out for 28-atom unit cells producing a number of dynamically stable high-pressure solutions with enthalpies below that of $cP7$. The best candidate

ground states were found to be $oS56$ (13–32 GPa range) and $tI56$ (above 32 GPa) favored by at least 60 meV/atom over $cP7$ at 30 GPa and dynamically stable in the 0–30 GPa range. The essential role of the crossover operation was shown by running an evolutionary search with just the mutation operation: neither $oS56$ nor $tI56$ were located in over 10^4 CG structural relaxations. CG optimization of 10^4 distorted $cP7$-CaB_6 supercells led to one $tI56$ hit demonstrating that incorporation of prior knowledge about the system can help locate the global minima without the need of advanced optimization methods. In fact, our tests in Ref. [31] show that with the unit cell parameters solved, the 28-atom $tI56$-CaB_6, 28-atom γ-B_{28}, or 44-atom $oC88$-Li ground states are found routinely with or without the crossover operation in only ~200 CG structural relaxations.

The plausibility of the lowest-enthalpy candidates was checked by comparing the respective XRD patterns. All the simulated $tI56$ peaks were present in each of the three collected patterns [Figs. 3(c)–3(e)] indicating that the laser-heating resulted in multiphase products with $tI56$ forming in all the cases. Since $tI56$ was predicted to stabilize around 30 GPa the remaining strong peaks at 31 and 34 GPa could be attributed to competing phase(s) stable at lower pressures. The conclusion was supported by the texture analysis of the raw 2D XRD image plate data: we found that the strong broad peak at 8.8 (12.9) degrees in Fig. 3(d) came from four (three) short smudged segments. Once the distinctive segments were masked (Figs. S7,S8 [31]) the remaining fairly uniform rings produced much sharper peaks around these 2θ angles (shown in green in Fig. 3(d)) consistent in magnitude and position with the reflections from $tI56$ [39].

The formation of several phases (with the smaller $tI56$ fraction at the lower pressures) could be one of the reasons for the lack of success in our first attempts to index the reflections. The ground state of CaB_6 under medium pressures (below 30 GPa) remains an open question: our best candidate structure, $oS56$, had well matching peaks at 5.6, 6.4, 8.9, 12.9, and 14 degrees but a number of simulated reflections were not present in the experimental pattern. We systematically explored other Ca-B compositions with an EA search and found no thermodynamic driver for CaB_6 to decompose [33]. Hence, determination of this stable form of CaB_6 may require further synthesis experiments at 20–25 GPa pressures or additional ground state search for even larger unit cells. The fact that both sets of peaks, from $tI56$ and the unknown phase(s), remained clearly visible down to ambient pressure (Fig. S3 [31]) indicates induced rebonding in the covalent network.

Examination of low-enthalpy structures identified in our CaB_6 ground state search revealed several rebonding pathways leading to considerable volume reduction. Fusion of two boron octahedra into twinned pentagonal bipyramids in the x-y planes [$oS28$ in Fig. 1(c)] was the most effective solution for small 14-atom unit cells; 21-atom unit cells had a framework of twinned bipyramids and regular octahedra resembling the layout in Na_3B_{20}; for 28-atom unit cells the bipyramid units preferred to distort to bridge across the layers. A more stable arrangement was achieved when half of the boron octahedra opened up and shared a bond to form strips [$oS56$ in Fig. 1(d)]. At higher pressures, four boron octahedra fused into interconnected 24-atom units [$tI56$ in Fig. 1(e)] which are among the largest known building blocks of boron [40]. Rationalization of the identified phases' stability and electronic properties is subject of futher study [33,41].

The discovery of the first non-$cP7$-type MB_6 compound quenched down to ambient pressure could help in the design of boron-based intermetallics with new electronic, magnetic, and superconducting properties through a careful choice of the metal and the synthesis conditions. Our ongoing calculations show that some of the identified high-pressure structures stabilize over $cP7$ in other MB_6 systems as well but each binary should be examined individually due to the observed richness of possible rebonding mechanisms. Methodologically, our study highlights the challenges in the search for new high-pressure polymorphs, even at a given composition. Laser heating in the DAC is essential for inducing structural transformations in covalent materials and can add complexity to the reaction products, e.g., with incomplete phase growth and diffuse scattering. Interpretation of observed XRD patterns can be aided by compound prediction methods but the determination of the true ground state(s) is never guaranteed due to the possible occurrence of crystal structures with an arbitrarily large number of formula units per cell. In this respect, available XRD reflection data play an important role as a stop criterion in the search for (meta)stable states [10]. The identification of the complex $tI56$-CaB_6 solution in our evolutionary search shows that it is possible to deal with increasingly large systems and unfamiliar structural motifs without *any* input of structural parameters from experiment.

A. N. K. and S. S. gratefully acknowledge the support of EPSRC (Grant No. CAF EP/G004072/1). E. R. M. was funded by Marie Curie IEF Project No. FP7-PEOPLE-2009-IEF-252586. A. N. K. thanks A. Sartbaeva for helpful discussions.

*Present address: Department of Earth Sciences, University of Oxford, South Parks Road, Oxford OX1 3AN, UK.

[1] M. I. McMahon and R. J. Nelmes, Chem. Soc. Rev. **35**, 943 (2006).
[2] C. J. Pickard and R. J. Needs, Nature Mater. **9**, 624 (2010).
[3] A. N. Kolmogorov and S. Curtarolo, Phys. Rev. B **74**, 224507 (2006).
[4] J. Feng, R. G. Hennig, N. W. Ashcroft, and R. Hoffmann, Nature (London) **451**, 445 (2008).
[5] P. F. McMillan, Nature Mater. **1**, 19 (2002).

[6] V. L. Solozhenko, O. O. Kurakevych, and A. R. Oganov, J. Superhard Mater. **30**, 428 (2008).
[7] A. R. Oganov, J. Chen, C. Gatti, Y. Ma, Y. Ma, C. W. Glass, Z. Liu, T. Yu, O. O. Kurakevych, and V. L. Solozhenko, Nature (London) **457**, 863 (2009).
[8] E. Y. Zarechnaya, L. Dubrovinsky, N. Dubrovinskaia, N. Miyajima, Y. Filinchuk, D. Chernyshov, and V. Dmitriev, Sci. Tech. Adv. Mater. **9**, 044209 (2008).
[9] M. Marques, M. I. McMahon, E. Gregoryanz, M. Hanfland, C. L. Guillaume, C. J. Pickard, G. J. Ackland, and R. J. Nelmes, Phys. Rev. Lett. **106**, 095502 (2011).
[10] A. R. Oganov, S. Ono, Y. Ma, C. W. Glass, and A. Garcia, Earth Planet. Sci. Lett. **273**, 38 (2008).
[11] S. W. Woodley and R. Catlow, Nature Mater. **7**, 937 (2008).
[12] C. J. Pickard and R. J. Needs, Phys. Rev. Lett. **97**, 045504 (2006).
[13] P. Baettig and E. Zurek, Phys. Rev. Lett. **106**, 237002 (2011).
[14] J. Lv, Y. Wang, L. Zhu, and Y. Ma, Phys. Rev. Lett. **106**, 015503 (2011).
[15] A. N. Kolmogorov, S. Shah, E. R. Margine, A. F. Bialon, T. Hammerschmidt, and R. Drautz, Phys. Rev. Lett. **105**, 217003 (2010).
[16] X. H. Ji, Q. Y. Zhang, J. Q. Xu, and Y. M. Zhao, Prog. Solid State Chem. **39**, 51 (2011).
[17] Y. Xu, L. Zhang, T. Cui, Y. Li, Y. Xie, W. Yu, Y. Ma, and G. Zou, Phys. Rev. B **76**, 214103 (2007).
[18] D. P. Young, D. Hall, M. E. Torelli, Z. Fisk, J. L. Sarrao, J. D. Thompson, H.-R. Ott, S. B. Oseroff, R. G. Goodrich, and R. Zysler, Nature (London) **397**, 412 (1999).
[19] J.-S. Rhyee and B. K. Cho, J. Appl. Phys. **95**, 6675 (2004).
[20] G. Allard, C.R. Acad. Sci. **T189**, 108 (1929).
[21] B. Albert and H. Hillebrecht, Angew. Chem., Int. Ed. **48**, 8640 (2009).
[22] P. Teredesai, D. V. S. Muthu, N. Chandrabhas, S. Meenakshi, V. Vijayakumar, P. Modak, R. S. Rao, B. K. Godwal, S. K. Sikka, and A. K. Sood, Solid State Commun. **129**, 791 (2004).
[23] M. Li, W. Yang, L. X. Li, H. X. Wang, S. W. Liang, and C. X. Gao, Physica (Amsterdam) **406B**, 59 (2011).
[24] B. K. Godwal, E. A. Petruska, S. Speziale, J. Yan, S. M. Clark, M. B. Kruger, and R. Jeanloz, Phys. Rev. B **80**, 172104 (2009).
[25] The full phonon dispersions were calculated with QUANTUM ESSPRESSO [26] using ultrasoft pseudopotentials (40 Ry energy cutoff). All final relative enthalpy values in Figs. 2(b) and 4 as well as the frequency versus pressure dependence in Fig. 2(a) were obtained with VASP [27] using the projector-augmented wave method [28] and treating the $2p$ states of Ca as semicore (500 eV energy cutoff). In both QUANTUM ESSPRESSO and VASP cases, we employed the Perdew-Burke-Ernzerhof parametrization [29] of the exchange-correlation functional in the generalized gradient approximation. Inclusion of vibrational entropy [30] for identified candidates at $T = 1500$ K was found to affect the $T = 0$ K relative stability by 20–30 meV/atom and the transition pressures by a few GPa. For further details see Ref. [31].
[26] P. Giannozzi *et al.*, J. Phys. Condens. Matter **21**, 395502 (2009).
[27] G. Kresse and J. Hafner, Phys. Rev. B **47**, 558 (1993);
G. Kresse and J. Furthmüller, *ibid.* **54**, 11169 (1996).
[28] P. E. Blöchl, Phys. Rev. B **50**, 17953 (1994).
[29] J. P. Perdew, K. Burke, and M. Ernzerhof, Phys. Rev. Lett. **77**, 3865 (1996).
[30] D. Alfè, Comput. Phys. Commun. **180**, 2622 (2009).
[31] See Supplemental Material at http://link.aps.org/supplemental/10.1103/PhysRevLett.109.075501 for a more detailed description of the experimental setup, XRD patterns, evolutionary search, simulation settings, and structural parameters of CaB_6 polymorphs.
[32] I. Popov, N. Baadji, and S. Sanvito, Phys. Rev. Lett. **108**, 107205 (2012).
[33] S. Shah and A. N. Kolmogorov (to be published).
[34] G. Mair, H. G. von Schnering1, M. Wörle, and R. Nesper, Z. Anorg. Allg. Chem. **625**, 1207 (1999).
[35] A. N. Kolmogorov, http://maise-guide.org.
[36] A. P. Hammersley, S. O. Svensson, M. Hanfland, A. N. Fitch, and D. Hüsermann, High Press. Res. **14**, 235 (1996).
[37] G. Bergerhoff and I. D. Brown, in *Crystallographic Databases*, edited by F. H. Allen *et al.* (International Union of Crystallography, Chester, 1987).
[38] A. Boultif and D. Louër, J. Appl. Crystallogr. **37**, 724 (2004).
[39] Note that the textured nature of the XRD data collected from the multiphase samples did not allow a reliable Rietveld refinement but we were able to carry out careful Le Bail fitting for all the pressure points. The fitted a and c lattice constants for $tI56$ were in excellent agreement with our calculated values (to within 0.5%) as shown in Fig. S5 [31].
[40] D. L. V. K Prasad, M. M. Balakrishnarajan, and E. D. Jemmis, Phys. Rev. B **72**, 195102 (2005).
[41] Analysis of the electronic properties of the proposed $oS56$ and $tI56$ will require a careful choice of the electronic structure method due to the known difficulty of describing the ~1 eV bandgap [42] in the relatively simple $cP7$-CaB_6 phase [43]. Indeed, the joint capacity of the bonding levels in $cP7$-MB_6 was shown over 50 years ago to be 20 electrons per boron octahedron (explaining why $cP7$-CaB_6 is a semiconductor) [44] but a number of DFT and GW calculations have failed to reproduce the compound's semiconducting state (a problem attributed to the bandgap sensitivity to the crystal structure parameters) [43]. Our first calculations suggest metallicity of the identified $oS56$ and $tI56$ phases: the generalized gradient approximation predicts the bottom of B-p-Ca-d nearly free electron bands to be pulled significantly below the Fermi level (by ~1 eV) and additional bands with predominantly B character to cross the Fermi level [33].
[42] S. Souma and T. Takahashi, J. Phys. Condens. Matter **19**, 355003 (2007).
[43] B. Lee and L.-W. Wang, Appl. Phys. Lett. **87**, 262509 (2005).
[44] H. C. Longuet-Higgins and M. de V. Roberts, Proc. R. Soc. A **224**, 336 (1954).